MODELING TRAFFIC VOLATILITY DYNAMICS IN AN URBAN NETWORK

Yiannis Kamarianakis*
Department of Economics, University of Crete and
Regional Analysis Division, Institute of Applied and Computational Mathematics,
Foundation for Research and Technology and Department of Economics, University of Crete.
IACM-FORTH, Vasilika Vouton, GR 71110, Heraklion Crete, Greece, Tel: +30 81 391771,
Fax: +30 81 391761, E-mail: kamarian@iacm.forth.gr

Angelos Kanas
Department of Economics, University of Crete, GR 74100, Rethymnon, Crete, Greece.
Tel: +30 28310 77427, Fax: +30 81 391761, E-mail: a-kanas@ermis.soc.uoc.gr

Poulicos Prastacos
Regional Analysis Division, Institute of Applied and Computational Mathematics,
Foundation for Research and Technology, Vasilika Vouton, GR 71110, Heraklion Crete,
Greece, Tel: +30 81 391767, Fax: +30 81 391761, E-mail: poulicos@iacm.forth.gr

Paper Submitted for Presentation and Publication at the 84th Transportation Research Board Annual Convention
Total Word Count: 6457

* Corresponding Author

MODELING TRAFFIC VOLATILITY IN AN URBAN NETWORK

Abstract. This article discusses the application of Generalized Auto-Regressive Conditional Heteroscedasticity (GARCH) time series models for representing the dynamics of traffic flow volatility. The methods encountered in the literature so far, focus on the levels of traffic flows while regarding variance constant through time. The approach adopted in this paper concentrates mostly on the autoregressive properties of traffic variability aiming to provide better confidence intervals for traffic flow forecasts. The model building procedure is illustrated using 7.5 min average traffic flow data for a set of eleven loop detectors located at major arterials that direct to the center of the city of Athens, Greece. A sensitivity analysis for coefficient estimates is undertaken, with respect to both time and space.

INTRODUCTION

Short term forecasting of traffic flow conditions has been for several years a hot topic of research as a means to support advanced traveler information and traffic management systems. Several forecasting techniques have been proposed which attempt to develop a mathematical framework based on theoretical or assumed empirical relationships. In this paper, we concentrate on statistical methods that aim to forecast the traffic flow conditions in an urban network at future time instants, based on real time data. Similar to the vast majority of the models presented in the literature so far, our methods are univariate in nature; historical traffic-flow data from a given location are used for modeling and predicting future behavior in the same location. Thus, in the univariate case, separate models are estimated for each measurement location (most usually loop detector) whereas in the multivariate case a single model is fitted to the whole dataset for the road network under study. Univariate models are flexible and can adapt to the specific characteristics of a distinct time series; on the other hand, multivariate models are expected to gain in accuracy through the incorporation of information taken from sites closely located to or with traffic flow patterns similar to the one being considered each time. Univariate specifications have ranged from Kalman filtering *(1),* non-parametric regression *(2),* regression with time varying coefficients *(3),* neural networks *(4)* and ARIMA models *(5, 6, 7, 8)*. For multivariate models that simultaneously describe traffic flow in various locations the interested reader is referenced to Stathopoulos and Karlaftis *(9)* and Kamarianakis and Prastacos *(10, 11, 12).*

To our knowledge, all previous modeling efforts concentrated only on traffic-flow levels but not on their variance that was assumed constant regardless of the state of traffic. However, it has been observed *(11)* that traffic conditions are much more volatile at some (heavy traffic/congestion) times than at others. Effective modeling of variance would produce more accurate confidence intervals for the forecasts; moreover, a variance that changes over time also has implications for the validity and efficiency of statistical inference about the parameters that describe the level of traffic flows. This article presents how the Generalized Auto-Regressive Conditional Heteroscedasticity (GARCH) time series models can be used to describe the time-dependent volatility structures of traffic conditions that are quite frequently observed in road networks. The adopted approach is illustrated through the investigation of traffic-flow dynamics for an extensive data set that corresponds to one month's data collected from loop detectors located at major arterials of the road network of Athens, Greece. GARCH coefficient estimation is done based on ARIMA models for traffic flow levels. The ARIMA models account for both short-term and periodic dynamics and have been proven to have superior forecasting performance for traffic flow levels relative to other methods, see *(11).* Thus, we combine both ARIMA and GARCH features expecting to be effective both for forecasting traffic flow levels and their confidence intervals.

In the next session, an overview of the GARCH model class is presented. Next, the experiment and the data are described followed by a report of the relevant model building details and an examination of the sensitivity of the model coefficient estimates both with respect to time (different subsets of the full data set) and to space (different measurement locations). Finally, we discuss the results and their implications for the applicability of GARCH modeling.

MODELING TRAFFIC VOLATILITY

The GARCH model class

One of the most prominent facts regarding traffic-flow dynamics is that volatility changes over time. In particular, periods of large movements alternate during the day with periods during which traffic conditions hardly change (see for example figures 2 and 3). This characteristic feature is referred to as *volatility clustering*. Even though the time-varying nature of traffic-flow volatility has been recognized, see for example (11), explicit modeling of the properties of the volatility process has not been taken up.

In this section we briefly discuss the class of GARCH models introduced by Engle *(13)* and Bollerslev *(14)*; for a thorough discussion the interested reader is referred to Hamilton *(15),* chapter 21. Nowadays, models from the GARCH class are the most popular volatility models among practitioners dealing with time series data. GARCH models enjoy such popularity because they are capable of describing not only the feature of volatility clustering, but also certain other characteristics of time series such as excess kurtosis or fat-tailedness. Over the past few years, quite a few nonlinear variants of the basic GARCH model have been proposed, most of them designed to capture such aspects as the asymmetric effect of positive and negative shocks on volatility, and possible correlation between the levels of the response variable and its volatility.

Observed traffic flows y_t can be written as the sum of a predictable and an unpredictable part,

$$y_t = E\left[y_t \mid \Omega_{t-1}\right] + \varepsilon_t \tag{1}$$

where Ω_{t-1} is the information set consisting of all relevant information up to and including time *t-1*. Research on statistical models for traffic-flow dynamics has been concentrated on different specifications for the predictable part or conditional mean $E\left[y_t \mid \Omega_{t-1}\right]$, while simply assuming that the unpredictable part or shock ε_t satisfies the white noise properties. In particular, ε_t was assumed to be both unconditionally and conditionally homoscedastic –that is, $E\left[\varepsilon_t^2\right] = E\left[\varepsilon_t^2 \mid \Omega_{t-1}\right] = \sigma^2$ for all *t*. This assumption can be relaxed so that the *conditional variance* of ε_t is allowed to vary over time –that is, $E\left[\varepsilon_t^2 \mid \Omega_{t-1}\right] = h_t$ for some nonnegative function $h_t \equiv h_t\left(\Omega_{t-1}\right)$. Put differently, ε_t is *conditionally heteroscedastic*. A convenient way to express this in general is

$$\varepsilon_t = z_t \sqrt{h_t} \tag{2}$$

where z_t is independent and identically distributed with zero mean and unit variance. For convenience we assume that z_t is described by a standard normal distribution.

From (2) and the properties of z_t it follows immediately that the distribution of ε_t conditional upon the history Ω_{t-1} is normal with mean zero and variance h_t. The *unconditional variance* of ε_t is still assumed to be constant though. Using the law of iterated expectations

$$\sigma^2 \equiv E\left[\varepsilon_t^2\right] = E\left[E\left[\varepsilon_t^2 \mid \Omega_{t-1}\right]\right] = E\left[h_t\right]. \quad (3)$$

Hence, we assume that the unconditional expectation of h_t is constant. To complete the model, we need to specify how the conditional variance of ε_t evolves through time.

Engle *(13)* introduced the class of Auto-Regressive Conditionally Heteroscedastic (ARCH) models to capture the volatility clustering of financial time series. In the basic ARCH model, the conditional variance of the shock that occurs at time *t* is a linear function of the squares of past shocks. For example, in the ARCH model of order 1, h_t is specified as,

$$h_t = \omega + \alpha_1 \varepsilon_{t-1}^2. \quad (4)$$

Obviously, the conditional variance h_t needs to be nonnegative. In order to guarantee that is the case for the ARCH(1) model, the parameters in (4) have to satisfy the conditions $\omega > 0$ and $a_1 \geq 0$. Where $a_1 = 0$, the conditional variance is constant and, hence, the series ε_t is conditionally homoscedastic. To understand why the ARCH model can describe volatility clustering, observe that (2) and (4) state that the conditional variance of ε_t is an increasing function of the shock that occurred in the previous time period. Therefore if ε_{t-1} is large (in absolute value), ε_t is expected to be large (in absolute value) as well. In other words, large (small) shocks tend to be followed by large (small) shocks of either sign.

To cope with the extended persistence of the empirical autocorrelation function, one may consider generalizations of the ARCH(1) model. One possibility to allow for more persistent autocorrelations is to include additional lagged squared shocks in the conditional variance function. The general ARCH(*q*) model is given by

$$h_t = \omega + \alpha_1 \varepsilon_{t-1}^2 + \alpha_2 \varepsilon_{t-2}^2 + ... + + \alpha_q \varepsilon_{t-q}^2. \quad (5)$$

To guarantee nonnegativeness of the conditional variance, it is required that $\omega > 0$ and $a_i \geq 0$ for all *i=1,...,q*. Adding ε_t^2 to both sides of (5) and moving h_t to the right hand side, the ARCH(*q*) model can be rewritten as an AR(*q*) model for ε_t^2,

$$\varepsilon_t^2 = \omega + a_1 \varepsilon_{t-1}^2 + ... + a_q \varepsilon_{t-q}^2 + v_t \quad (6)$$

where $v_t = \varepsilon_t^2 - h_t$. It follows that the unconditional variance of ε_t is equal to

$$\sigma^2 = \frac{\omega}{1 - a_1 - ... - a_q}. \quad (7)$$

To capture the dynamic patterns in conditional volatility adequately by means of an ARCH(*q*) model, *q* often needs to be taken quite large. It turns out that it can be quite cumbersome to estimate the parameters in such a model, because of the nonnegativity and stationarity conditions that need to be imposed. As an alternative solution, Bollerslev *(14)*

suggested adding lagged conditional variances to the ARCH model instead. For example, adding h_{t-1} to the ARCH(1) model (4) results in the Generalized ARCH (GARCH) model of order (1,1)

$$h_t = \omega + a_1 \varepsilon_{t-1}^2 + \beta_1 h_{t-1} . \tag{8}$$

The parameters in this model should satisfy $\omega > 0$, $a_1 > 0$ and $\beta_1 \geq 0$ to guarantee that $h_t \geq 0$ while a_1 must be strictly positive for β_1 to be identified.

To see why the lagged conditional variance avoids the necessity of adding many lagged squared residual terms in the model, notice that (8) can be rewritten as

$$h_t = \omega + a_1 \varepsilon_{t-1}^2 + \beta_1 \left(\omega + a_1 \varepsilon_{t-2}^2 + \beta_1 h_{t-2} \right), \tag{9}$$

or, by continuing the recursive substitution, as

$$h_t = \sum_{i=1}^{\infty} \beta_1^i \omega + a_1 \sum_{i=1}^{\infty} \beta_1^{i-1} \varepsilon_{t-i}^2 . \tag{10}$$

This shows that the GARCH(1,1) model corresponds to an ARCH(∞) model with a particular structure for the parameters of the lagged ε_t^2 terms.

The general GARCH(*p,q*) model is given by

$$h_t = \omega + \sum_{i=1}^{q} a_i \varepsilon_{t-i}^2 + \sum_{i=1}^{p} \beta_i h_{t-i} = \omega + a(L) \varepsilon_t^2 + \beta(L) h_t . \tag{11}$$

where $a(L) = a_1 L + ... + a_q L^q$ and $\beta(L) = \beta_1 L + ... + \beta_p L^p$ and L is the backshift operator that transforms an observation of a time series to the previous one ($L\varepsilon_t = \varepsilon_{t-1}$ and it is trivial to see that $L^p \varepsilon_t = \varepsilon_{t-p}$). As before, by adding ε_t^2 to both sides of (11) and moving h_t to the right hand side, the GARCH(*p,q*) model can be interpreted as an ARMA(*m,p*) model for ε_t^2 given by

$$\varepsilon_t^2 = \omega + \sum_{i=1}^{m} \left(a_i + \beta_i \right) \varepsilon_{t-i}^2 - \sum_{i=1}^{p} \beta_i v_{t-i} + v_t , \tag{12}$$

where $m = \max\left(p, q\right)$, $a_i \equiv 0$ for $i > q$, $\beta_i \equiv 0$ for $i > p$ and again $v_t = \varepsilon_t^2 - h_t$. To determine the appropriate orders *p* and *q* in the GARCH(*p,q*) model one can use a general-to-specific procedure by starting with a model with *p* and *q* set equal to large values, and testing down using likelihood ratio type of restrictions. Alternatively, one may use penalized likelihood criteria like the Akaike's information criterion that is used in the application that follows. For optimal GARCH order selection issues the interested reader is referenced to Hamilton *(15)*, chapter 21.

THE APPLICATION

The study area

The urban area of Athens, the capital of Greece, has an area of 60 km^2 and a population of approximately four million people. Total daily demand for travel is about 5.5 million trips with about 1 million occurring during the 2-hour peak period *(9)*. In the last ten years traffic flows have been increasing by about 3.5% annually. Travel times in such a congested network can be very long and the potential for travel-time savings through Intelligent Transportation Systems Technologies are high.

A set of 88 loop detectors (figure 1) has been installed by the Ministry of Environment and Public Works at major roads of the Athens network to measure traffic volume and road occupancy (approximated by the time occupancy of each loop detector). Measurements take place every 90 seconds and are immediately transmitted to the Urban Traffic Control Center where they are used by the Siemens MIGRA traffic control system to adjust streetlights timing. An indicator of data quality ranging from 1 to 3 is transmitted as well since often electronic or system failures result in measurements that might not be accurate.

The data analyzed

In this study, we model a dataset provided by eleven loop detectors (highlighted in figure 1) located at major arterials leading to the center of the city. The total number of loops located at streets with direction towards the center of Athens is thirty-six. Twenty-five of them provided data of high quality at the period of our study; the eleven loops we use are a subset of these twenty-five.

The variable under study is the relative velocity, defined as the traffic volume divided by the road occupancy. This is a variable more volatile than the other two, but it reflects in a clear way the traffic condition. As indicated by Rice and van Zwet *(3)*, multiplied by a constant related to the average vehicle length it can provide a proxy for the average space-mean speed.

A typical period –in terms of traffic flow- was selected to be studied: from February 11, 2002 to March 10, 2002, from 7 a.m. to 9 p.m. Observations corresponding to weekends were discarded since traffic flow patterns differ significantly these days. The initial dataset contained a time series of 21210 observations for every loop detector. To ease implementation and smooth out noise, averages (of the flow/occupancy ratio) over five consecutive 90-second intervals were taken, thus resulting in a total of 2126 observations per detector, 112 measurements per day for each loop.

Table 1 presents the basic statistical measures for relative and differenced velocities for the loops under study. As depicted in figures 2, 3 and the lower part of figure 4, volumes, occupancies and relative velocities, follow a quasi-sinusoidal pattern with daily period and time dependent variation. The latter is more evident from the time series plots of de-trended relative velocities. De-trending was applied via differencing; differenced relative velocities express the difference of what is observed in a loop today to what was observed yesterday at the same time. Occupancies tend to follow a bimodal distribution and this feature is

transferred to relative velocities (see for example the case of loop 1 in figure 4). Both figure 4 and table 1 indicate that differenced relative velocities are closer to the normal distribution than relative velocities (the normal distribution has both skewness and kurtosis equal to zero).

Model fitting

The first step of the modeling stage was to estimate ARIMA models for the *conditional mean* of relative velocities. ARIMA models should be applied to stationary variables and relative velocities are clearly non-stationary as evident from figure 3. The daily periodicity can be removed by differencing (of order 112 since we have 112 observations per day); the same strategy was followed by Smith et al. *(16)*. Transformation to (mean) stationarity practically implies that the variable finally modeled is the daily increment in relative velocity.

In *(11)* it is shown that factored ARIMA models that account for both short-term and periodic dynamics lead to superior short-term forecasting performance when compared to other -multivariate, namely Vector Autoregressive Moving Average (VARMA) and Space-Time ARIMA- model classes. The model formulation they used is

$$(1-\phi_1 B)y_t = (1-\theta_1 B)(1-\theta_{112})\varepsilon_t \tag{13}$$

where $\phi_1, \theta_1, \theta_{112}$ are coefficients that need to be estimated, and *B* is the back-shift operator. Here, to ease comparison with the GARCH models that are estimated next, we estimate equivalent models (not so parsimonious since they contain one more parameter) in their conventional ARIMA form

$$y_t = a_1 y_{t-1} + \varepsilon_t + \beta_1 \varepsilon_{t-1} + \beta_2 \varepsilon_{t-112} + \beta_3 \varepsilon_{t-113} \tag{14}$$

where $a_1, \beta_1, \beta_2, \beta_3$ are unknown coefficients.

Maximum likelihood estimation results for the eleven measurement locations of the study are shown in table 2, where columns two to five correspond to estimates for $a_1, \beta_1, \beta_2, \beta_3$ respectively; t-statistics indicating statistical significance of estimations are shown in parentheses. To highlight model stability we also present estimations that correspond to the first 75% and 50% of observations in time. Similarly to *(11),* the most significant terms appear to be the autoregressive one (a_1), and the moving average that corresponds to periodic dynamics (β_2). It is remarkable that although differenced relative velocities are characterized by completely different distributions their evolution in time is well described by single model form. Finally, we note that residual autocorrelations were found to be non-significant practically for all models, indicating that the proposed ARIMA formulation is well specified. Autocorrelation plots are omitted at this point for space economy; they are available from the authors upon request.

Next, based on the ARIMA specification we used maximum likelihood to estimate the following regression model with autocorrelated disturbances

$$\begin{aligned} y_t &= b_1 y_{t-1} + v_t \\ v_t &= c_1 v_{t-1} + c_2 v_{t-112} + c_3 v_{t-113} + \varepsilon_t \end{aligned} \tag{15}$$

and performed the Lagrange multiplier test proposed by *(13)* for ARCH disturbances. Since in every case the tests rejected the null hypothesis of non-ARCH disturbances we estimated various GARCH formulations; as common in many applications GARCH(1,1) provided the most adequate representation of volatility. (15) in this case transforms to

$$\begin{aligned} y_t &= b_1 y_{t-1} + v_t \\ v_t &= c_1 v_{t-1} + c_2 v_{t-112} + c_3 v_{t-113} + \varepsilon_t \\ \varepsilon_t &= \sqrt{h_t} e_t \\ h_t &= \omega + k\varepsilon_{t-1}^2 + d h_{t-1} \end{aligned} \tag{16}$$

Columns two to eight at table 3 contain estimates for $b_1, c_1, c_2, c_3, \omega, k, d$ respectively. In all cases k and d yield a sum close to 1 with k small and d large. This implies that the impact of shocks on the conditional variance diminishes only very slowly. A comparison of model fit statistics with the ones in table 2 indicates that we obtain a slightly worse fit in levels compared to the ARIMA models. It seems that to get accurate confidence limits one should sacrifice some forecasting accuracy on the levels of traffic flows.

CONCLUSIONS AND DIRECTIONS FOR FURTHER RESEARCH

This study demonstrated the application of GARCH model class in an urban network using data sets originating from a set of loop detectors. The results obtained demonstrate that traffic flow dynamics display time dependent volatility. In forecasting applications, the challenging issue is not only to forecast the levels of traffic flows but to provide accurate confidence bands for the forecasts as well. This can be achieved via modeling the autoregressive structure of volatility.

This is only a first step towards traffic flow volatility modeling. The methodology should be further refined via allowing for possible nonlinear GARCH structures where positive and negative shocks have asymmetric effects. Moreover it is challenging to incorporate volatility modeling in space-time models where a single model is fitted to the whole set of loop detector measurements.

REFERENCES

1. Whittaker, J., S. Garside, and K. Lindveld. Tracking and predicting a network traffic process. *International Journal of Forecasting,* Vol. 13*,* 1997, pp. 51-61.

2. Davis, G.A., and N.L. Nihan. Nonparametric regression and short-term freeway traffic forecasting. *ASCE Journal of Transportation Engineering,* Vol. 117(2), 1991, pp. 178-188.

3. Rice, J., and E. van Zwet. A simple and effective method for predicting travel times on freeways. *IEEE Intelligent Transportation Systems Proceedings*, 2001.

4. Van Lint, J.W.C., S.P. Hoogendoorn, and H.J. van Zuylen. Freeway travel time prediction with state-space neural networks: Modeling State-Space dynamics with recurrent neural networks. In *Transportation Research Record: Journal of the Transportation Research Board, No. 1811,* TRB, National Research Council, Washington D.C., 2002, pp. 30-39.

5. Williams, B.M., P.K. Durvasula, and D.E. Brown. Urban freeway travel prediction: application of seasonal ARIMA and Exponential Smoothing Models. *77th Annual Transportation Research Board Meeting*, 1997.

6. Lee, S., and D.B. Fambro. Application of subset autoregressive integrated moving average model for short-term freeway traffic volume forecasting. *Transportation Research Record 1678*, 1999.

7. Williams, B.M. Multivariate vehicular traffic flow prediction: an evaluation of ARIMAX modeling. *80th Annual Transportation Research Board Meeting,* 2001.

8. Yang, F., Y. Zhaozheng, H.X. Liu,, and B. Ran. An on-line recursive short-term traffic prediction algorithm. *83rd Annual Transportation Research Board Meeting*, 2004.

9. Stathopoulos, A., and G.M. Karlaftis. A multivariate state-space approach for urban traffic flow modeling and prediction. *81th Annual Transportation Research Board Meeting*, 2002.

10. Kamarianakis, Y., and P. Prastacos. Space-time modeling of traffic flow. *Methods of spatial analysis – spatial time series analysis, ERSA Proceedings*, Dortmund, September, 2002.

11. Kamarianakis, Y., and P. Prastacos. Forecasting traffic flow conditions in an urban network: Comparison of univariate and multivariate approaches. . In *Transportation Research Record: Journal of the Transportation Research Board, No. 1857,* TRB, National Research Council, Washington D.C., 2003, pp. 74-84.

12. Kamarianakis, Y., and P. Prastacos. Bivariate traffic relations: A space-time modeling approach. Article submitted for publication. Available at http://www.iacm.forth.gr/regional/people/kamarianakis.html.

13. Engle, R.F. Autoregressive conditional heteroscedasticity with estimates of the variance of United Kingdom inflation. *Econometrica,* Vol. 50, 1981, pp. 987-1007.

14. Bollerslev, T. Generalized autoregressive conditional heteroscedasticity. *Journal of Econometrics,* Vol. 72, 1986, pp. 117-133,.

15. Hamilton, J.D. Time Series Analysis. Princeton University Press, 1994.

16. Smith, B.L., B.M. Williams, and R.K. Oswald. Comparison of parametric and nonparametric models for traffic flow forecasting. *Transportation Research Part C*, Vol 10(4), 2002, pp. 303-321.

LIST OF TABLES

LIST OF FIGURES

LOOP	MEAN	VARIANCE	SKEWNESS	KURTOSIS	MIN	MAX
V1	1.7599	2.0975	1.0279	-0.4519	0	5.7568
V4	1.4948	0.2244	-0.7783	0.9613	0	3.1194
V7	1.5304	1.0707	1.0788	-0.0349	0	4.8780
V8	1.5666	0.1140	0.1452	-0.3065	0.6954	2.7176
V11	3.9104	1.7291	-0.7660	-0.3330	0.5427	6.1951
V12	1.4002	1.3672	1.4002	1.1357	0.1601	5.8571
V14	0.9545	0.1992	2.8920	12.4167	0.1938	4.6250
V16	1.3211	0.1620	0.9529	2.3527	0.1290	3.6292
V60	1.0025	0.1197	-0.9323	0.4830	0.0144	1.7660
V67	0.8984	0.2849	-0.0029	-1.2277	0	2.1277
V86	0.8613	0.1291	0.2162	-0.5852	0.1111	2.3333
V1DIF	-0.0310	3.5022	0.0554	0.3100	-5.4667	4.7240
V4DIF	0.0094	0.4307	0.0555	0.8715	-2.8873	2.1200
V7DIF	-0.0058	1.2003	0.0094	1.5757	-3.7810	3.9978
V8DIF	0.0020	0.1408	-0.0694	0.2411	-1.4258	1.2736
V11DIF	0.0274	2.4752	0.0611	0.2748	-4.3801	5.0083
V12DIF	0.0590	2.0337	0.0240	1.7938	-5.1166	4.9337
V14DIF	0.0150	0.3656	0.1151	7.9573	-3.7586	3.6941
V16DIF	0.0054	0.2831	0.0433	1.6348	-2.6040	2.3411
V60DIF	-0.0039	0.1876	0.0186	1.0103	-1.3797	1.6159
V67DIF	0.0154	0.3487	-0.1170	0.1074	-1.8387	1.8144
V86DIF	0.0068	0.2124	0.0575	-0.1273	-1.3929	1.6012

TABLE 1 Summary statistics for relative velocities and differenced relative velocities.

	AR1	MA1	MA112	MA113	AIC	St. Err.	Variance
Loop 1	**0.789** (51.18)	**-0.198** (-7.94)	**0.878** (45.65)	**0.152** (6.06)	**4689**	**0.743**	**0.552**
Loop1 (75%)	0.766 (40.74)	-0.221 (-7.55)	0.851 (33.07)	0.169 (5.69)	3550	0.762	0.580
Loop 1 (50%)	0.767 (35.65)	-0.223 (-5.59)	0.994 (1.04)	0.228 (1.08)	2260	0.695	0.484
Loop 4	**0.865** (55.97)	**0.442** (15.76)	**0.928** (35.17)	**-0.410** (-13.73)	**1794**	**0.358**	**0.128**
Loop4 (75%)	0.856 (45.57)	0.444 (13.27)	0.932 (18.93)	-0.403 (-10.12)	1476	0.370	0.137
Loop 4 (50%)	0.858 (37.85)	0.468 (11.24)	0.911 (12.46)	-0.384 (-7.24)	1008	0.373	0.139
Loop 7	**0.834** (52.66)	**0.253** (8.92)	**0.936** (31.84)	**-0.243** (-8.37)	**3487**	**0.543**	**0.295**
Loop7 (75%)	0.854 (49.72)	0.318 (9.84)	0.903 (24.11)	-0.256 (-7.48)	2434	0.516	0.266
Loop 7 (50%)	0.860 (42.77)	0.341 (8.46)	0.924 (9.85)	-0.270 (-5.27)	1621	0.513	0.263
Loop 8	**0.748** (16.65)	**0.564** (10.11)	**0.815** (43.57)	**-0.448** (-9.09)	**653**	**0.276**	**0.076**
Loop8 (75%)	0.717 (13.06)	0.514 (7.58)	0.902 (24.58)	-0.496 (-7.82)	447	0.264	0.070
Loop 8 (50%)	0.747 (14.25)	0.509 (7.28)	0.972 (5.75)	-0.537 (-4.78)	273	0.247	0.061
Loop 11	**0.826** (47.92)	**0.289** (9.81)	**0.848** (47.05)	**-0.242** (-8.64)	**5079**	**0.823**	**0.678**
Loop11 (75%)	0.828 (43.13)	0.255 (7.63)	0.825 (33.33)	-0.209 (-6.44)	3816	0.838	0.702
Loop 11 (50%)	0.839 (39.30)	0.232 (5.80)	0.898 (12.01)	-0.198 (-4.41)	2477	0.812	0.660
Loop 12	**0.838** (62.07)	**0.006** (0.24)	**0.988** (8.09)	**0.006** (0.24)	**3832**	**0.580**	**0.336**
Loop12 (75%)	0.815 (47.09)	-0.019 (-0.63)	0.893 (27.14)	0.018 (0.60)	2756	0.577	0.333
Loop 12 (50%)	0.793 (35.29)	-0.008 (-0.20)	0.915 (12.07)	0.060 (1.52)	1962	0.615	0.379
Loop 14	**0.772** (36.44)	**0.291** (8.81)	**0.930** (28.55)	**-0.220** (-6.58)	**1632**	**0.343**	**0.118**
Loop14 (75%)	0.770 (29.10)	0.357 (8.67)	0.945 (15.45)	-0.302 (-6.77)	697	0.283	0.080
Loop 14 (50%)	0.737 (20.41)	0.320 (5.80)	0.921 (9.75)	-0.241 (-4.13)	644	0.307	0.094
Loop 16	**0.602** (18.83)	**0.107** (2.68)	**0.891** (41.93)	**-0.067** (-1.79)	**1568**	**0.341**	**0.117**
Loop16 (75%)	0.585 (15.44)	0.086 (1.84)	0.870 (30.04)	-0.055 (-1.29)	1130	0.335	0.112
Loop 16 (50%)	0.488 (9.38)	0.015 (0.23)	0.969 (4.73)	0.016 (0.26)	897	0.344	0.118
Loop 60	**0.737** (31.13)	**0.218** (6.39)	**0.838** (47.80)	**-0.169** (-5.32)	**438**	**0.261**	**0.068**
Loop60 (75%)	0.721 (25.87)	0.176 (4.44)	0.796 (33.49)	-0.132 (-3.61)	396	0.266	0.071
Loop 60 (50%)	0.697 (19.64)	0.155 (3.09)	0.807 (17.84)	-0.067 (-1.41)	281	0.263	0.069
Loop 67	**0.590** (18.40)	**0.084** (2.10)	**0.932** (32.30)	**-0.071** (-1.85)	**1993**	**0.376**	**0.141**
Loop67 (75%)	0.510 (12.66)	-0.020 (-0.43)	0.900 (25.48)	0.019 (0.43)	1463	0.372	0.139
Loop67 (50%)	0.668 (15.97)	0.200 (3.54)	0.874 (13.96)	-0.219 (-4.03)	1024	0.381	0.145
Loop 86	**0.795** (29.57)	**0.511** (13.29)	**0.933** (31.97)	**-0.482** (-12.35)	**1167**	**0.306**	**0.093**
Loop86	0.804	0.550	0.990	-0.540	938	0.301	0.091

(75%)	(26.17)	(12.23)	(3.15)	(-3.01)			
Loop 86 (50%)	0.835 (24.12)	0.613 (11.56)	0.959 (5.27)	-0.572 (-4.61)	630	0.300	0.090

TABLE 2 Coefficient estimates and model fit statistics for the ARIMA models.

	LAGDEP	ERR1	ERR112	ERR113	ARCH0	ARCH1	GARCH1	AIC	MSE	Tot. R^2
Loop 1	**0.787** (42.54)	**-0.188** (-5.02)	**0.500** (45.84)	**-0.096** (-4.25)	**0.067** (11.17)	**0.305** (17.29)	**0.695** (39.43)	**5060**	**0.764**	**0.781**
Loop1 (75%)	0.745 (27.29)	-0.217 (-4.45)	0.523 (40.29)	-0.090 (-3.05)	0.074 (9.00)	0.306 (13.24)	0.694 (30.00)	3792	0.785	0.773
Loop 1 (50%)	0.737 (19.34)	-0.223 (-3.67)	0.578 (34.02)	-0.089 (-2.11)	0.054 (7.21)	0.311 (12.38)	0.689 (27.40)	2310	0.735	0.771
Loop 4	**0.760** (53.75)	**0.311** (10.89)	**0.505** (28.49)	**0.1524** (6.26)	**0.003** (4.04)	**0.105** (7.00)	**0.895** (59.41)	**2283**	**0.183**	**0.576**
Loop4 (75%)	0.764 (47.91)	0.314 (9.49)	0.512 (23.70)	0.150 (5.10)	0.003 (3.10)	0.102 (6.16)	0.898 (54.43)	1805	0.197	0.571
Loop 4 (50%)	0.789 (36.81)	0.365 (11.13)	0.520 (17.12)	0.184 (5.06)	0.0001 (0.74)	0.020 (3.17)	0.981 (159.70)	1184	0.202	0.569
Loop 7	**0.764** (49.35)	**0.148** (5.03)	**0.503** (44.22)	**0.079** (3.71)	**0.036** (16.12)	**0.383** (21.61)	**0.618** (34.89)	**3581**	**0.431**	**0.641**
Loop7 (75%)	0.794 (50.86)	0.164 (5.80)	0.478 (38.35)	0.107 (4.90)	0.025 (13.25)	0.404 (23.33)	0.596 (34.39)	2326	0.376	0.664
Loop 7 (50%)	0.826 (46.30)	0.226 (8.46)	0.449 (23.53)	0.131 (4.32)	0.018 (8.17)	0.362 (14.48)	0.639 (25.58)	1490	0.388	0.659
Loop 8	**0.556** (23.14)	**0.394** (15.45)	**0.5171** (25.89)	**0.211** (8.69)	**8E-24** (0.00)	**5E-5** (0.02)	**1** (467.51)	**1046**	**0.098**	**0.305**
Loop8 (75%)	0.549 (19.70)	0.390 (13.06)	0.533 (23.23)	0.213 (7.40)	2E-23 (0.00)	1E-8 (0.00)	1 (23062)	754	0.097	0.307
Loop 8 (50%)	0.539 (15.10)	0.299 (7.16)	0.550 (19.64)	0.212 (5.52)	-1E-20 (0.00)	1E-8 (0.01)	1 (674946)	439	0.092	0.329
Loop 11	**0.770** (43.29)	**0.249** (8.40)	**0.535** (30.46)	**0.130** (5.22)	**0.023** (4.76)	**0.123** (9.38)	**0.876** (66.50)	**5599**	**0.908**	**0.633**
Loop 11 (75%)	0.794 (45.11)	0.189 (6.68)	0.496 (23.22)	0.093 (3.40)	3E-5 (0.91)	1E-8 (0.00)	1 (8123)	4118	0.936	0.655
Loop 11 (50%)	0.828 (35.19)	0.204 (4.32)	0.480 (18.63)	0.112 (3.00)	0.072 (4.79)	0.274 (8.22)	0.726 (21.78)	2639	0.929	0.686
Loop 12	**0.836** (79.5)	**0.114** (3.77)	**0.474** (39.44)	**0.062** (2.75)	**0.067** (19.16)	**0.381** (15.76)	**0.564** (31.38)	**3960**	**0.515**	**0.747**
Loop 12 (75%)	0.839 (62.77)	0.098 (2.72)	0.430 (31.31)	0.026 (0.98)	0.071 (15.06)	0.318 (12.12)	0.576 (23.61)	2780	0.470	0.747
Loop 12 (50%)	0.825 (43.19)	0.103 (2.21)	0.518 (26.68)	0.034 (0.90)	0.056 (10.56)	0.301 (9.57)	0.638 (24.03)	1921	0.551	0.727
Loop 14	**0.703** (30.94)	**0.231** (7.73)	**0.616** (67.88)	**0.189** (7.77)	**0.019** (13.58)	**0.422** (20.81)	**0.578** (28.50)	**1637**	**0.168**	**0.542**
Loop 14 (75%)	0.635 (19.50)	0.221 (5.89)	0.548 (48.92)	0.161 (5.89)	0.021 (7.21)	0.197 (8.17)	0.625 (16.16)	827	0.114	0.458
Loop 14 (50%)	0.648 (16.39)	0.251 (5.07)	0.591 (40.89)	0.198 (5.20)	0.025 (5.88)	0.199 (6.44)	0.622 (12.63)	690	0.134	0.463
Loop 16	**0.553** (14.00)	**0. 050** (1.10)	**0.503** (31.01)	**0.029** (0.98)	**0.009** (6.19)	**0.235** (9.81)	**0.765** (31.87)	**1895**	**0.157**	**0.445**
Loop 16 (75%)	0.516 (11.13)	0.025 (0.47)	0.500 (25.20)	(0.027) (0.79)	0.018 (3.89)	0.119 (5.11)	0.765 (16.55)	1315	0.150	0.414
Loop 16 (50%)	0.484 (7.45)	0.013 (0.18)	0.470 (19.17)	(0.028) (0.62)	0.029 (3.08)	0.135 (3.95)	0.703 (9.36)	1022	0.178	0.391
Loop 60	**0.699** (32.58)	**0.203** (6.60)	**0.503** (27.90)	**0.146** (6.00)	**0.001** (3.33)	**0.080** (7.60)	**0.921** (88.10)	**852**	**0.089**	**0.525**
Loop 60 (75%)	0.675 (28.54)	0.160 (4.32)	0.488 (22.75)	0.093 (3.25)	0.035 (3.99)	0.161 (4.13)	0.457 (3.90)	606	0.090	0.535
Loop 60 (50%)	0.675 (22.31)	0.136 (2.82)	0.456 (15.53)	0.105 (2.70)	0.050 (3.32)	0.159 (3.33)	0.281 (1.51)	396	0.090	0.503
Loop 67	**0.531** (15.2)	**0.034** (0.76)	**0.498** (25.36)	**0.002** (0.09)	**0.003** (3.74)	**0.089** (8.34)	**0.911** (85.62)	**2475**	**0.200**	**0.423**
Loop 67 (75%)	0.505 (11.33)	-0.005 (-0.08)	0.482 (20.93)	0.004 (0.11)	0.035 (2.84)	0.092 (3.44)	0.728 (8.81)	1752	0.195	0.416
Loop 67 (50%)	0.584 (14.80)	0.107 (2.03)	0.484 (15.96)	0.036 (0.98)	0.053 (3.04)	0.151 (3.32)	0.592 (5.13)	1158	0.204	0.381
Loop 86	**0.576** (22.35)	**0.244** (8.21)	**0.486** (23.51)	**0.153** (5.97)	**-2E-21** (0.00)	**1E-8** (0.00)	**1** (3508)	**1765**	**0.140**	**0.340**
Loop 86 (75%)	0.538 (16.42)	0.225 (6.11)	0.483 (19.52)	0.140 (4.56)	0.138 (20.28)	0.052 (1.55)	4.73E-24 0	1357	0.145	0.322

Loop 86 (50%)	0.559 (14.29)	0.260 (6.00)	0.444 (13.73)	0.184 (4.74)	0.134 (15.84)	0.083 (1.80)	4.73E-20 0	874	0.146	0.304

TABLE 3 Coefficient estimates and model fit statistics for the GARCH models.

FIGURE 1 Loop detectors at the Athens road network. The ones used in this study are highlighted with different color and a label.

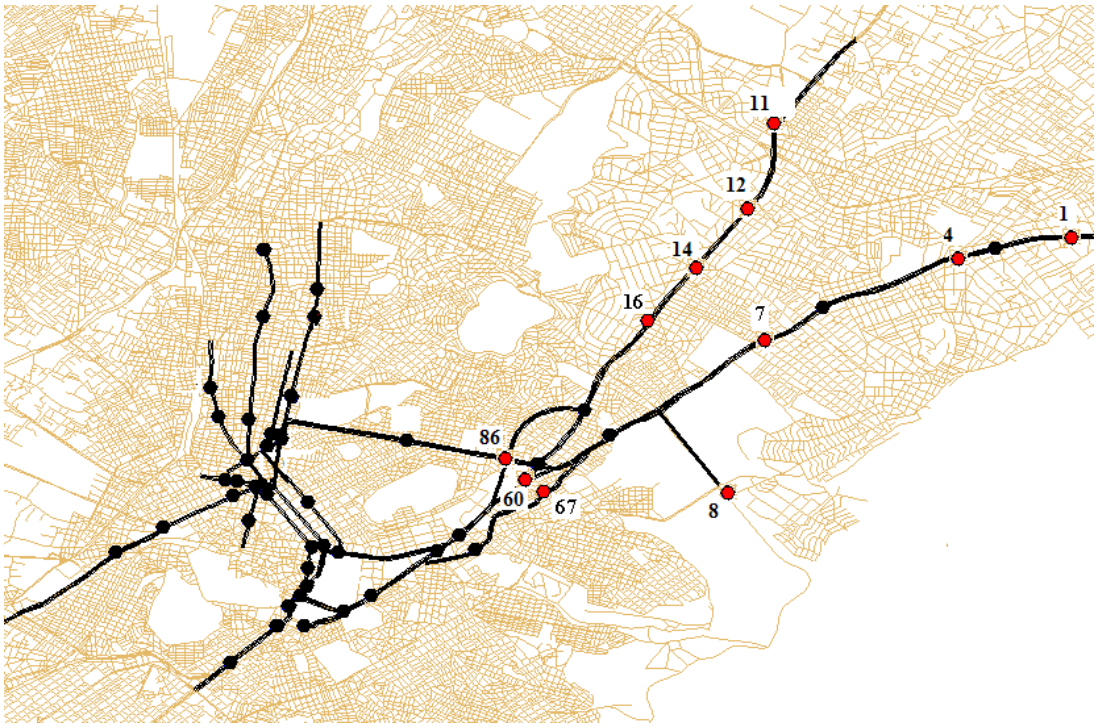

FIGURE 2 Evolution of traffic volumes and road occupancies through time for the 11 loop detectors.

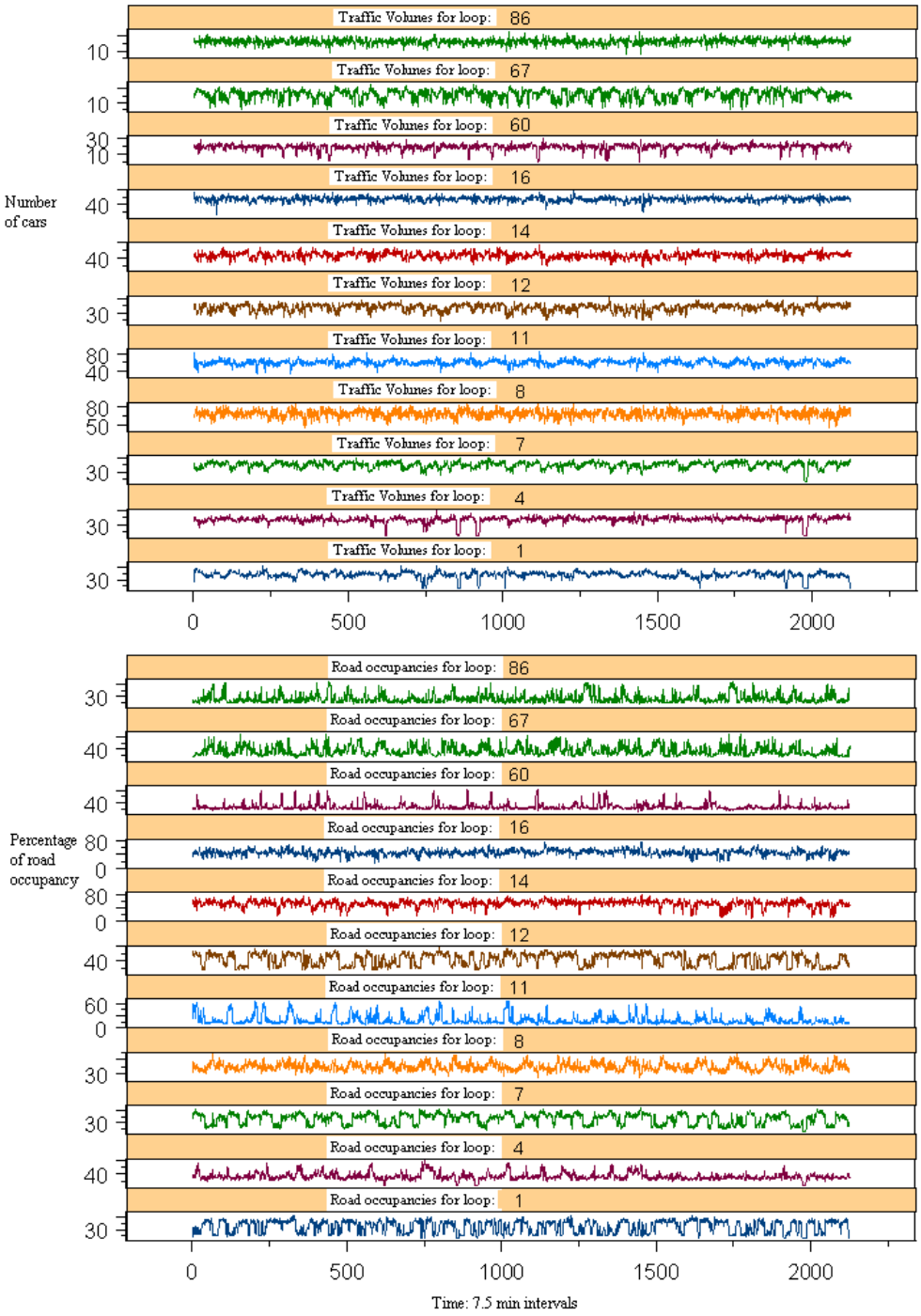

FIGURE 3 Evolution of relative velocities and differenced relative velocities through time for the 11 loop detectors

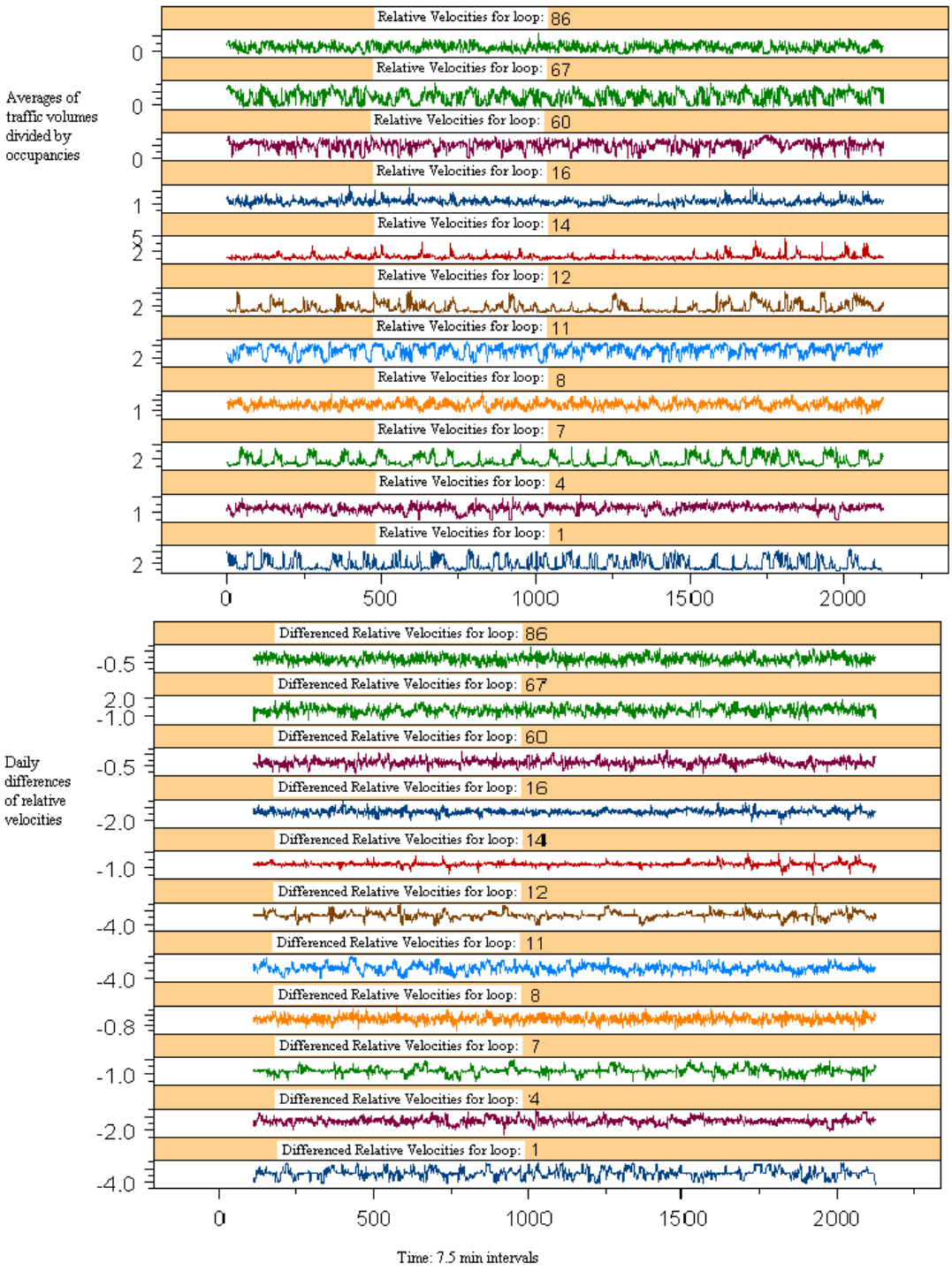

FIGURE 4 Density plots for Volumes, Occupancies, Relative Velocities and Differenced Relative Velocities for loop 1 and a zoom in (observations corresponding to one week) for relative velocities